Visible-Light Photoredox-Catalyzed C–O Bond Cleavage of Diaryl Ethers by Acridinium Photocatalysts at Room Temperature

Fang-Fang Tan
Xi'an Jiaotong University
Xiao-Ya He He
Xi'an Jiaotong University
Wan-Fa Tian
Xi'an Jiaotong University
Yang Li (liyang79@mail.xjtu.edu.cn)
Xi'an Jiaotong University https://orcid.org/0000-0003-4724-4785

Article

Keywords:

Posted Date: August 7th, 2020

DOI: https://doi.org/10.21203/rs.3.rs-52259/v1

Version of Record: A version of this preprint was published at Nature Communications on November 30th, 2020. See the published version at https://doi.org/10.1038/s41467-020-19944-x.

Abstract

We have developed visible-light photoredox-catalyzed C–O bond cleavage of diaryl ethers by an acidolysis with an aryl car-boxylic acid and a following one-pot hydrolysis. Two phenols are obtained from a diaryl ether at room temperature. The aryl carboxylic acid used for the acidolysis can be recovered. The key to success of the acidolysis is merging visible-light photore-dox catalysis with a new acridinium photocatalyst and Lewic acid catalysis with Cu(TMHD)2. Preliminary mechanistic studies indicate that the catalytic cycle occurs via a rare selective electrophilic attack of the generated aryl carboxylic radical on the electron-rich aryl ring of diphenyl ether. This transformation is applied to a gram-scale reaction and the model of 4-O-5 lignin linkages.

Background

We have developed visible-light photoredox-catalyzed C–O bond cleavage of diaryl ethers by an acidolysis with an aryl carboxylic acid and a following one-pot hydrolysis. Two phenols are obtained from a diaryl ether at room temperature. The aryl carboxylic acid used for the acidolysis can be recovered. The key to success of the acidolysis is merging visible-light photoredox catalysis with a new acridinium photocatalyst and Lewic acid catalysis with $Cu(TMHD)_2$. Preliminary mechanistic studies indicate that the catalytic cycle occurs via a rare selective electrophilic attack of the generated aryl carboxylic radical on the electron-rich aryl ring of diphenyl ether. This transformation is applied to a gram-scale reaction and the model of 4-O-5 lignin linkages.

Biomass widely distributes in nature containing lignin as one of major components.[1-3] In lignin, there are three major types of aryl ether bonds of α-O-4 (218 kJ/mol), β-O-4 (289 kJ/mol), and 4-O-5 (314 kJ/mol).[1-3] Cleavage of C–O bonds in lignin can afford renewable aryl sources for fine chemicals. However, the high bond energies of these C–O bonds, especially the 4-O-5-type diary ether C–O bonds, make the cleavage very challenging.[1-10] Therefore, in fundamental research, cleavage of aryl C–O bonds has attracted much attention.[11-18]

Cleavage of the α-O-4 and β-O-4 types of C–O bonds has been studied, even under mild conditions by visible-light photoredox catalysis.[19-23] For cleavage of the 4-O-5-type diary ether C–O bonds, classical studies focused on the hydrolysis by supercritical water, the hydrogenolysis with poor selectivity using the model of 4-O-5 lignin linkages. [2,4-5,10] Many aryl skeletons were destroyed. In selective cleavage methods, the use of stoichiometric alkali metals[24-26] or electrocatalytic hydrogenolysis[27-29] limited the large-scale applications because of the associated high costs.

In recent years, the selective hydrogenolysis under comparatively milder conditions was developed by Hartwig, Grubbs, Wang, et al (Fig. 1A).[30-41] The hydrogenolysis was accomplished by using [Ni], [Fe], or [Co] as catalyst, with H_2 (1–6 bar) or $LiAlH_4$ (2.5 equiv) as reductant at 120–180 °C.[30-36] A higher than stoichiometric strong base, such as NaO^tBu/KO^tBu/KHMDS (2.5 equiv), is important for the selectivity

(Fig. 1A, conditions a). Without using transition-metal catalyst, a combination of Et_3SiH/NaH (³2.5 equiv) and KHMDS (2.5 equiv) at 140–165 °C achieved the selective hydrogenolysis (Fig. 1A, conditions b).[37-38] More importantly, by MOF or Pd/C as catalyst without a base, the selective hydrogenolysis with H_2 (10–30 bar) at 120–200 °C obtained no more than 55% yield (Fig. 1A, conditions c).[39-41] In these studies, a large amount of reductant, strong base, and/or the low yield are/is still the limited factor(s) for the applications.

Thus, there exists a strong incentive to develop more practical methods for diaryl ether C–O bonds cleavage, toward the utilization of lignin as renewable aryl sources.

Herein, we describe visible-light photoredox-catalyzed C–O bond cleavage of diaryl ethers by an acidolysis with an aryl carboxylic acid and a following one-pot hydrolysis at room temperature (rt). Two phenols, with some advantages than arenes in transformations such as aminations, the functionalization, cross coupling reactions,[42-43] are obtained. The aryl carboxylic acid used for the acidolysis can be recovered (Fig. 1B). The key to success of the acidolysis is merging visible-light photoredox catalysis with a new acridinium photocatalyst (PC) and Lewis acid catalysis with $Cu(TMHD)_2$ (Fig. 1B). Inspired by the significant contributions of Fukuzumi,[44-46] Nicewicz,[47-49] Sparr,[50-51] et al.[52-54] on acridinium PCs, we investigated the use of a new acridinium catalyst. Notably, an aryl ring with electron-withdrawing groups, instead of mesitylene, typically used in other acridinium catalysts,[44-54] on the 9-position resulted in obviously higher efficiency. Furthermore, with this method, the model of 4-O-5 lignin linkages afforded phenol and 2-methoxyphenol in high efficiency. Compared with the developed selective hydrogenolysis in recent years, using H_2O instead of a large amount of reductant afforded two more valuable phenols at rt.

We developed the C–O bond cleavage of diaryl ethers containing a carboxylic acid group on the ortho position by a visible-light photoredox-catalyzed intramolecular aryl migration from an aryl ether to the ortho carboxylic acid group at rt, and a following one-pot hydrolysis.[55] Thus, we envisioned the possibility of C–O bond cleavage of general diaryl ethers by an aryl acidolysis with an aryl carboxylic acid followed by a hydrolysis, which would expand the scope of the special diaryl ethers largely, even to the model of 4-O-5 lignin linkages.

Specifically, in the aryl acidolysis, photoredox catalysis affords an aryl carboxylic radical **A**, then followed by its electrophilic attack on the diphenyl ether, and a single electron transfer (SET) with a proton and an electron (Fig. 2). However, the two issues make the transformation more challenging. First, although some intramolecular electrophilic attack of aryl carboxylic acid radicals to arenes has been reported,[55-60] the intermolecular electrophilic attack of aryl carboxylic acid radicals to arenes has not been successfully explored. The intermolecular electrophilic attack of aryl carboxylic acid radicals to arenes was proposed in thermal decomposition of substituted dibenzoyl peroxides in diphenyl ether, in which the corresponding aryl benzoates were obtained in less than 39% yields with low selectivity. In addition, in comparison with the produced aryl carboxylic acid radicals, the amount of arenes was huge because diphenyl ether was

used as solvent.[61] Second, similarly to the intramolecular reaction, the formation of the more stable ester C–O bond should be the driving force of the diaryl ether C–O cleavage, as the C–O bond energies of an aryl ether and an ester are about 78.8 and 87–93 kcal mol^{-1}, respectively.[62-63] However, the possible intermediate **B** is indicated to lack stronger driving force of C–O bond cleavage, compared with the six-membered ring intermediate in the intramolecular reaction.[55-60] As mentioned below, less than 10% product with the remained starting material was obtained under the optimized reaction conditions for intramolecular reactions (Table 1, entries 1, 2). Perhaps a Lewis acid could activate the ether.

Results And Discussion

Optimization study. With these considerations in mind, diphenyl ether (**1a**) and 4-methylbenzoic acid (**2a**) were studied as model substrates. Under our developed conditions for the intramolecular C–O bond cleavage,[55] using PDI[64] or Acr^+-Mes ClO_4^- (**PC 1**)[44-46] as PC, with 10 mol% K_2HPO_4 as base, under 450–455 nm blue LEDs irradiation, only less than 10% of phenyl 4-methylbenzoate (**3a**) and phenol (**4a**) were obtained (Table 1, entries 1, 2). Thereafter, a series of Lewis acids such as $Cu(OAc)_2$, $Cu(acac)_2$, $Cu(OTf)_2$, $Ni(acac)_2$, $Fe(acac)_2$, $Zn(acac)_2$, and $Cu(TMHD)_2$ were studied (Table S1, entries 1–6, Table 1, entry 3). $Cu(TMHD)_2$ slightly promoted the transformation. Adjustment of the wavelength of the blue LEDs to the maximum absorption of **PC 1 (**425–430 nm) induced a slightly increased reactivity (Table 1, entry 4). Other solvents such as MeOH, DCE, EtOAc, and acetone did not give any better results (Table S1, entries 7–10). As Acr^+-Mes ClO_4^- is susceptible to degradation in the presence of oxygen-centered radicals,[48] and de-N-methylation is also possible,[47] it is deduced that the generated carboxylic acid radical may induce the degradation of Acr^+-Mes ClO_4^-.

Subsequently, **PC 2** and **PC 3** were tried,[48] in which the N-phenyl were used instead of the N-methyl, and also with the tert-butyl on the 3- and 6-positions of the acridinium in the latter case. Both factors induced distinct higher efficiency (Table 1, entries 5 and 6, **3a** in 29% and 55%, with **4a** in 22% and 49%).

Furthermore, the influence of the substitutes on the 9-aryl ring was investigated. Since the complex procedure for synthesis of **PC 3**,[48] **PC 4**–**PC 9**, with a similar skeleton to that of **PC 3** but with different substituents on the 9-aryl ring, by a two-step synthetic procedure,[52] were investigated (Table 1, entries 7–12). Notably, the aryl rings with electron-withdrawing groups instead of mesitylene, typically used in other acridinium catalysts,[44-54] resulted in noticeably high efficiencies. To our delight, **PC 9** with 2'-Cl and 4'-F on the 9-aryl ring resulted in 80% of **3a** with 71% of **4a** (entry 12). Although the smaller group of 2'-Cl compared with the methyl groups in mesitylene was used, X-ray crystallography of **PC 9** unambiguously confirmed the angle of torsion between the 9-aryl ring and the acridinium ring (Fig. 1B), which is closely related with a longer fluorescence lifetime.[44,47] In addition, variation of the tert-butyl groups from the 2,7-positions to the 3,6-positions resulted in decreased efficiency (entry 13). Further variation of the substituents on the 10-aryl ring revealed that the unsubstituted phenyl gave a slightly higher yield (entry 15). Decreasing the amount of $Cu(TMHD)_2$ resulted in obviously lower efficiency (entry 16). The amount

of base did not influence the reaction efficiency, even without base (entries 17, 18). Other Lewis acids, such as $Cu(OAc)_2$, $Cu(acac)_2$, and $Fe(acac)_2$ instead of $Cu(TMHD)_2$, were investigated once again (entries 19–22), as slight differences during the initial investigation. The distinctly positive influence of $Cu(TMHD)_2$ was further confirmed. Without base and $Cu(TMHD)_2$, no reactivity was observed (entry 23). Control experiments indicate that a PC and visible light irradiation are essential (entries 25, 26). The fluorescence lifetime and the redox potentials of **PC 1**–**PC 12** were determined (Table S2). The data do not provide clear insight regarding the higher efficiency achieved using **PC 9**.

Table 1 Optimization of the Reaction Conditions.

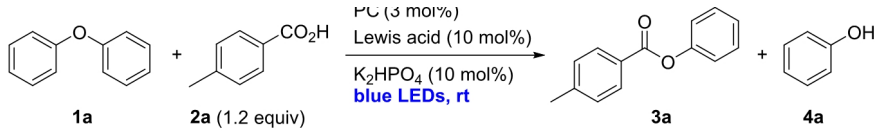

1a **2a** (1.2 equiv) **3a** **4a**

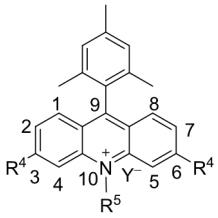

PC 1: R^4=H, R^5=Me,Y^-=ClO_4^-
PC 2: R^4=H, R^5=Ph, Y^-=BF_4^-
PC 3: R^4=^{t}Bu, R^5=Ph, Y^-=BF_4^-

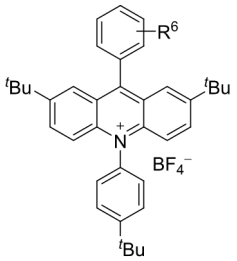

PC 4: R^6=2',4',6'-tri-CH_3 **PC 7**: R^6=4'-F
PC 5: R^6=3',5'-di-CH_3 **PC 8**: R^6=2',4'-di-Cl
PC 6: R^6=4'-CF_3 **PC 9**: R^6=2'-Cl-4'-F

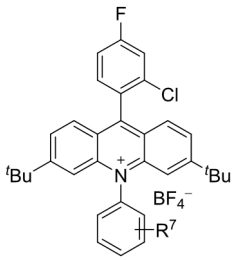

PC 10: R^7=4'-^{t}Bu,
PC 11: R^7=2',4',6'-tri-CH_3
PC 12: R^7=H

entry	Lewis acid	PC	wavelength (nm)	**3a** yield (%)	**4a** yield (%)[f]
1	—	PDI	450–455	<5	<5
2	—	**PC 1**	450–455	8	<5
3	$Cu(TMHD)_2$	**PC 1**	450–455	11	10
4	$Cu(TMHD)_2$	**PC 1**	425–430	15	10
5	$Cu(TMHD)_2$	**PC 2**	425–430	29	22
6	$Cu(TMHD)_2$	**PC 3**	425–430	55	49
7	$Cu(TMHD)_2$	**PC 4**	425–430	46	41
8	$Cu(TMHD)_2$	**PC 5**	425–430	60	50
9	$Cu(TMHD)_2$	**PC 6**	425–430	67	62
10	$Cu(TMHD)_2$	**PC 7**	425–430	74	65
11	$Cu(TMHD)_2$	**PC 8**	425–430	77	67
12	$Cu(TMHD)_2$	**PC 9**	425–430	80	71
13	$Cu(TMHD)_2$	**PC 10**	425–430	63	59
14	$Cu(TMHD)_2$	**PC 11**	425–430	50	48
15	$Cu(TMHD)_2$	**PC 12**	425–430	71	69
16[b]	$Cu(TMHD)_2$	**PC 9**	425–430	47	45
17[c]	$Cu(TMHD)_2$	**PC 9**	425–430	78	70
18[d]	$Cu(TMHD)_2$	**PC 9**	425–430	80(76)[g]	70(69)[g]
19[d]	$Cu(OAc)_2$	**PC 9**	425–430	48	38
20[d]	$Cu(acac)_2$	**PC 9**	425–430	56	47
21[d]	$Ni(acac)_2$	**PC 9**	425–430	13	9
22[d]	$Fe(acac)_2$	**PC 9**	425–430	21	19
23[d]	—	**PC 9**	425–430	—	—
24	—	**PC 9**	425–430	12	7
25[d]	$Cu(TMHD)_2$	—	425–430	—	—
26[d,e]	$Cu(TMHD)_2$	**PC 9**	425–430	—	—

[a]Reaction condtions: **1a** (0.24 mmol), **2a** (0.2 mmol), PC (3.0 mol%), Lewis acid (10 mol%), solvent (2.0 mL), irradiation with blue LEDs for 30 h, ^{1}H NMR yields of **3a** and **4a** were reported by using $Cl_2CHCHCl_2$ as an internal standard.
[b]$Cu(TMHD)_2$ (5 mol%).
[c]K_2HPO_4 (5 mol%).
[d]Without base.
[e]In dark.
[f]Due to the volatility of phenol (during work-up), phenol was obtained in slightly lower yields than **3a**.
[g]Isolated yield.

Evaluation of substrate scope. With the optimized reaction conditions, the substrate scope was investigated (Fig. 3). First, the influence of various substituents on the benzoic acid was investigated. 4-Methoxy, 4-tert-butyl gave decreased reaction efficiencies (**3ab**, **3ac** in 61–65% with **4a** in 56–60%). The benzoic acid afforded **3ad** in 55% with **4a** in 50%. 4-Fluoro, 4-chloro, and 4-bromo induced excellent yields (**3ae**–**3ag** in 87–91% with **4a** in 82–84%). 4-Nitro, 4-aldehyde also resulted in high efficiencies (**3ah**, **3ai** in 71–77% with **4a** in 65–70%). The substituents on the 3-position were also studied. As with the substituents on the 4-position, fluoro and chloro resulted in high yields (**3ak**, **3al** in 81–86% with **4a** in

74–76%). Methyl gave a decreased yield (**3aj** in 61%). When the methyl was installed on the 2-position, no product was observed. 2-Fluoro resulted in lower efficiency (**3ap** in 63%). The phenomenon should be influenced by the steric factor.

Next, the substituents on the aryl ring of the diphenyl ethers were investigated (Fig. 4). With electron-withdrawing groups such as methyl ester, trifluoromethyl, nitro, cyan, or acetyl on the 4-position of the aryl ring, **3a** (65–74%) and the corresponding phenols with these electron-withdrawing groups (**4b**-**4f**, 62–72%) were selectively obtained in high yields. The results agree with the designed pathway of the electrophilic attack of the generated carboxylic acid radical, including the selective attack on the electron-rich aryl ring of the diphenyl ethers. 4-Bromo afforded two esters **3a** (22%) and **3aq** (64%), and two phenols **4g** (21%) and **4a** (54%). The reason for the result may be the synergic effect of induction and conjugation of the bromo. For the 4-phenyl group, **3ar** and **4a** were selectively obtained in 84% yields. The reason for the selectivity may be the 4-phenyl group stabilizing the generated radical intermediate after the electrophilic attack. 4-Methyl and 4-methoxy resulted in very low efficiency (<10%). Generally, it maybe be explained by their comparatively lower oxidation potentials, inhibiting generation of the aryl carboxylic radical (Table S3). Methyl, methoxyl, dimethyl substituents on other positions afforded **3as**–**3au** in 68–80% yields, and comparable yields of **4a**. Symmetric dimethyl, dimethoxyl, dibromo, and dichloro, and asymmetric dichloro on the 3- or 4-positions resulted in good to high efficiencies (**3av**, **3aw**, 52–90%, **4h**–**4k**, 50–86%). When the methyl and methoxy on 2- or 3-position, with 4¢-ester, 4¢-cynao or 4¢-trifluoro, were investigated, the esters with methyl or methoxyl, as well as phenols with these electron-withdrawing groups, were obtained selectively in high yields (**3as**–**3ax**, 72–82%, **4b**, **4e**, **4c**, 70–82%).

Synthetic application. To demonstrate the potential application, a gram-scale reaction of **1a** with **2e** in a flow reactor and a following one-pot hydrolysis was conducted. **4a** was obtained in 80% yield, with **2e** in 88% recovery rate (Fig. 5A). Meanwhile, the model of 4-O-5 lignin linkage (**1t**)[30] afforded **4a** (71%) and **4l** (75%) in high efficiency, with **2e** in 82% recovery rate (Fig. 5B).

Mechanism studies. To gain insight into the reaction mechanism, a series of experiments were conducted. First, UV–vis absorption spectra of each component and the reaction mixture confirmed that **PC 9** acts as a PC (Fig. 6A). Second, luminescent quenching experiments were conducted (Fig. 6B). The anion of **2a** (4-MePhCO$_2^-$*n*Bu$_4$N$^+$), **2a**, and **1a** quenched the excited state **PC 9***. The anion of **2a** displayed an obviously larger quenching rate. Third, the pH value of the reaction mixture was determined as 3.61 or 4.30, with or without 10 mol% Cu(TMHD)$_2$. Based on these pH values, Cu(TMHD)$_2$ should promote the ionization of **2a** by the salt effect.[65] In addition, under base free conditions, the high reactivity of 80% ester **3a** with Cu(TMHD)$_2$ (entry 18), and 13–56% ester **3a** with Cu(OAc)$_2$, Cu(acac)$_2$, Ni(acac)$_2$, Fe(acac)$_2$ (entries 19–22) in comparison with no production of **3a** without any these metal salts (entry 23), these results suggest that the function of Cu(TMHD)$_2$ also as a Lewis acid to promote the transformation.

Furthermore, with addition of TEMPO as oxidant, compounds **5**, instead of **3** and **4**, were obtained via the possible intermediates **C**[48] (Fig. 7). This result suggests the generation of intermediate **B'** to afford **3a** and **4a** under the optimized conditions.

The thermodynamic feasibility of the photo-induced SET was analyzed based on the oxidation–reduction potentials. The oxidation potential of $E^{4\text{-CH3PhCO2}\bullet/4\text{-CH3PhCO2}-}$, $E^{\mathbf{1a}+\bullet/\mathbf{1a}}$, and the reduction potential of $E^{\mathbf{PC\ 9/PC\ 9}-\bullet}$ in CH_3CN were determined as +1.45 V vs. SCE, +1.86 V vs. SCE[66], and −0.47 V vs. SCE (Figures S9, S10, and S34), respectively. The excited-state energy $E_{0,0}$ of **PC 9** was determined as 2.63 eV (Fig. S22). Therefore, the reduction potential of $E^{\mathbf{PC\ 9}*/\mathbf{PC\ 9}-\bullet}$ was calculated as + 2.16 V vs. SCE ($E^{PC*/PC-\bullet}=E^{PC/PC-\bullet}+E_{0,0}$) (Fig. S34). These reduction potentials indicate the prior formation of $PC^{-\bullet}$ and the carboxylic acid radical[55-60] by a SET between PC* and the carboxylic acid anion. Furthermore, a quantum yield value of φ=0.20 was determined. Thus, at this stage, whether the reaction proceeds via a photoredox catalytic pathway or a radical chain pathway could not be reached.[67]

Based on these results, the reaction mechanism is proposed as shown in Fig. 8. First, $Cu(TMHD)_2$ promotes the ionization of **2a** to afford $\mathbf{2a}^-$ and a proton. Meanwhile, irradiation of PC with blue LEDs leads to the excited state PC*. A SET occurs between PC* and $\mathbf{2a}^-$ to generate the carboxylic acid radical **Aȼ** and $PC^{-\bullet}$. An electrophilic attack of **Aȼ** occurs on the electron-rich aryl ring of diphenyl ethers to form intermediate **Bȼ**. A SET between **Bȼ** and $PC^{-\bullet}$ in the presence of a proton, and the promotion of $Cu(TMHD)_2$ as a Lewis acid afford **3a**, **4a**, with the regeneration of PC.

In summary, we have developed visible-light photoredox-catalyzed C–O bond cleavage of diaryl ethers by an acidolysis and a following one-pot hydrolysis at rt. Two phenols are obtained from a diaryl ether in high efficiency. The aryl carboxylic acid used for the acidolysis can be recovered. The key to success of the acidolysis is merging visible-light photoredox catalysis with a new acridinium photocatalyst and Lewis acid catalysis with $Cu(TMHD)_2$. The transformation is applied to a gram-scale reaction and the model of 4-O-5 lignin linkages. In comparison with the developed selective hydrogenolysis in recent years, using H_2O instead of a large amount of reductant affords two more valuable phenols at rt. This approach would inspire further visible-light photoredox-catalyzed C–O bond cleavage of 4-O-5 lignin linkages in native biomass for utilization of lignin as renewable aryl sources.

Methods

General Procedure for the C-O Bond Cleavage of Diaryl Ethers. To a quartz tube equipped with a magnetic stirring bar, **PC 9** (0.015 mmol, 3.0 mol%, 9.60 mg), compound **1** (0.50 mmol), compound **2** (0.60 mmol), ($Cu(TMHD)_2$) (0.05 mmol, 10 mol%, 21.5 mg) were added. The tube was evacuated and filled with argon three times with each cycle in 15 minutes. Freshly distilled solvent was then added into the tube via a syringe under argon atmosphere, then stirred and irradiated with 425-430 nm blue LEDs at ambient temperature (19-21 °C) in a Wattecs Parallel Reactor (Figure S1) for 30-60 h. After the reaction, the solvent

was removed in vacuo and the residue was purified by column chromatography (petroleum ether/EtOAc = 200/1 - 5/1) to afford compound **3** and **4**.

Full experimental procedures are provided in the Supplemental Information.

Data availability

The X-ray crystallographic coordinates for structures reported in this study have been deposited at the Cambridge Crystallographic Data Centre (CCDC), under deposition number 2004336. These data can be obtained free of charge from The Cambridge Crystallographic Data Centre via https://www.ccdc.cam.ac.uk/. The data supporting the findings of this study are available within the article and its Supplementary Information files. Any further relevant data are available from the authors on request.

Declarations

Author Contributions

F.-F. Tan and X.-Y. He performed the experiments and analyzed the data, F.-F. Tan and W.-F. Tian conducted the theoretical studies. Y. Li directed the project and wrote the manuscript.

Conflict of interest

The authors declare no conflict of interest.

Acknowledgements

This work was supported by National Key R&D Program of China (Nos: 2018YFB1501601) and the Instrument Analysis Center of the Xi'an Jiaotong University. We thank Prof. Gang He, Xi'an Jiaotong University for the support on cyclic voltammetry experiments and emission-quenching experiments.

References

1. Zhang, Z., Song, J. & Han, B. Catalytic transformation of lignocellulose into chemicals and fuel products in ionic liquids. *Chem. Rev.* **117**, 6834–6880 (2017).
2. Zakzeski, J., Bruijnincx, P. C. A., Jongerius, A. L. & Weckhuysen, B. M. The catalytic valorization of lignin for the production of renewable chemicals. *Chem. Rev.* **110**, 3552–3599 (2010).
3. Sun, Z., Fridrich, B., de Santi, A., Elangovan, S. & Barta, K. Bright side of lignin depolymerization: toward new platform chemicals. *Chem. Rev.* **118**, 614–678 (2018).
4. Siskin, M., Katritzky, A. R. & Balasubramanian, M. Aqueous organic chemistry. 4. cleavage of diaryl ethers. *Energ. Fuel.* **5**, 770–771 (1991).

5. He, J., Zhao, C. & Lercher, J. A. Ni-catalyzed cleavage of aryl ethers in the aqueous phase. *J. Am. Chem. Soc.* **134**, 20768–20775 (2012).
6. Shuai, L. et al. Formaldehyde stabilization facilitates lignin monomer production during biomass depolymerization, *Science* **354**, 329–333 (2016).
7. Wiensch, E. M. & Montgomery, J. Nickel-catalyzed amination of silyloxyarenes through C-O bond activation. *Angew. Chem. Int. Ed.* **57**, 11045–11049 (2018)
8. Wang, M., Gutierrez, O. Y., Camaioni, D. & Lercher, J. A. Palladium catalyzed reductive insertion of alcohols in aryl ether bonds. *Angew. Chem. Int. Ed.* **57**, 3747–3751 (2018).
9. Sun, Z. et al. Complete lignocellulose conversion with integrated catalyst recycling yielding valuable aromatics and fuels. *Nat. Catal.* **1**, 82–92 (2018).
10. Hua, M. et al. Ru/hydroxyapatite as a dual-functional catalyst for efficient transfer hydrogenolytic cleavage of aromatic ether bonds without additional bases. *Green Chem.* **21**, 5073–5079 (2019).
11. Kakiuchi, F., Usui, M., Ueno, S., Chatani, N. & Murai, S. Ruthenium-catalyzed functionalization of aryl carbon-oxygen bonds in aromatic ethers with organoboron compounds. *J. Am. Chem. Soc.* **126**, 2706–2707 (2004).
12. Guan, B. T., Wang, Y., Li, B. J., Yu, D. G. & Shi, Z. J. Biaryl construction via Ni-catalyzed C-O activation of phenolic carboxylates. *J. Am. Chem. Soc.* **130**, 14468–14470 (2008).
13. Tobisu, M., Shimasaki, T. & Chatani, N. Nickel-catalyzed cross-coupling of aryl methyl ethers with aryl boronic esters. *Angew. Chem. Int. Ed.* **47**, 4866–4869 (2008).
14. Correa, A. & Martin, R. Ni-catalyzed direct reductive amidation via C-O bond cleavage. *J. Am. Chem. Soc.* **136**, 7253–7256 (2014).
15. Zhao, Y. & Snieckus, V. Beyond directed ortho metalation: Ru-catalyzed C-Ar-O activation/cross-coupling reaction by amide chelation. *J. Am. Chem. Soc.* **136**, 11224–11227 (2014).
16. Ackerman, L. K., Lovell, M. M. & Weix, D. J. Multimetallic catalysed cross-coupling of aryl bromides with aryl triflates. *Nature* **524**, 454–457 (2015).
17. Cong, X., Tang, H. & Zeng, X. Regio- and chemoselective Kumada-Tamao-Corriu reaction of aryl alkyl ethers catalyzed by chromium under mild conditions. *J. Am. Chem. Soc.* **137**, 14367–14372 (2015).
18. Tay, N. E. S. & Nicewicz, D. A. Cation radical accelerated nucleophilic aromatic substitution via organic photoredox catalysis. *J. Am. Chem. Soc.* **139**, 16100–16104 (2017).
19. Zhang, C. & Wang, F. Catalytic lignin depolymerization to aromatic chemicals. *Acc. Chem. Res.* **53**, 470–484 (2020).
20. Nguyen, J. D., Matsuura, B. S. & Stephenson, C. R. J. A photochemical strategy for lignin degradation at room temperature. *J. Am. Chem. Soc.* **136**, 1218–1221 (2014).
21. Luo, N. et al. Photocatalytic oxidation-hydrogenolysis of lignin β-O-4 models via a dual light wavelength switching strategy. *ACS Catal.* **6**, 7716–7721 (2016).
22. Wu, X. et al. Solar energy-driven lignin-first approach to full utilization of lignocellulosic biomass under mild conditions. Nat. Catal. 1, 772–780 (2018).

23. Han, P. et al. Promoting Ni(II) catalysis with plasmonic antennas. *Chem*, **5**, 2879–2899 (2019).
24. Sartoretto, P. A. & Sowa, F. J. The cleavage of diphenyl ethers by sodium in liquid ammonia. I. ortho and para substituted diphenyl ethers. *J. Am. Chem. Soc.* **59**, 603–606 (1937).
25. Weber, F. C. & Sowa, F. J. The cleavage of diphenyl ethers by sodium in liquid ammonia. III. 4,4'-disubstituted diphenyl ethers. *J. Am. Chem. Soc.* **60**, 94–95 (1938).
26. Maercker, A. Ether cleavage with organo-alkali-metal compounds and alkali metals. *Angew. Chem. Int. Ed.* **26**, 972–990 (1987).
27. Thornton, T. A., Woolsey, N. F. & Bartak, D. E. Carbon-oxygen bond-cleavage reactions by election-transfer. 3. electrochemical formation and decomposition of the diphenyl ether radical-anion. *J. Am. Chem. Soc.* **108**, 6497–6502 (1986).
28. Pierre D., André C., Jean L., Louis B. & Hugues M. Electrocatalytic hydrogenation of 4-phenoxyphenol on active powders highly dispersed in a reticulated vitreous carbon electrode, *Can. J. Chem.* **77**, 1225–1229 (1999).
29. Wu, W. B. & Huang, J. M. Electrochemical cleavage of aryl ethers promoted by sodium borohydride. *J. Org. Chem.* **79**, 10189–10195 (2014).
30. Sergeev, A. G. & Hartwig, J. F. Selective, Nickel-catalyzed hydrogenolysis of aryl ethers. *Science* **332**, 439–443 (2011).
31. Sergeev, A. G., Webb, J. D. & Hartwig, J. F. A heterogeneous Nickel catalyst for the hydrogenolysis of aryl ethers without arene hydrogenation. *J. Am. Chem. Soc.* **134**, 20226–20229 (2012).
32. Zaheer, M., Hermannsdörfer, J., Kretschmer, W. P., Motz, G. & Kempe, R. Robust heterogeneous Nickel catalysts with tailored porosity for the selective hydrogenolysis of aryl ethers. *ChemCatChem* **6**, 91–95 (2014).
33. Gao, F., Webb, J. D. & Hartwig, J. F. Chemo- and regioselective hydrogenolysis of diaryl ether C-O bonds by a robust heterogeneous Ni/C catalyst: applications to the cleavage of complex lignin-related fragments. *Angew. Chem. Int. Ed.* **55**, 1474–1478 (2016).
34. Saper, N. I. & Hartwig, J. F. Mechanistic investigations of the hydrogenolysis of diaryl ethers catalyzed by Nickel complexes of N-heterocyclic carbene ligands. *J. Am. Chem. Soc.* **139**, 17667–17676 (2017).
35. Ren, Y., Yan, M., Wang, J., Zhang, Z. C. & Yao, K. Selective reductive cleavage of inert aryl C-O bonds by an iron catalyst. *Angew. Chem. Int. Ed.* **52**, 12674–12678 (2013).
36. Ren, Y.-L. et al. Highly selective reductive cleavage of aromatic carbon–oxygen bonds catalyzed by a cobalt compound. *Catal. Commun.* **52**, 36–39 (2014).
37. Fedorov, A., Toutov, A. A., Swisher, N. A. & Grubbs, R. H. Lewis-Base silane activation: from reductive cleavage of aryl ethers to selective ortho-silylation. *Chem. Sci.* **4**, 1640–1645 (2013).
38. Xu, H. et al. Reductive cleavage of C-O bond in model compounds of lignin. *Chin. J. Chem.* **35**, 938–942 (2017).

39. Stavila, V. et al. MOF-Based catalysts for selective hydrogenolysis of carbon–oxygen ether bonds. *ACS Catal.* **6**, 55–59 (2016).
40. Stavila, V. et al. IRMOF-74(n)-Mg: a novel catalyst series for hydrogen activation and hydrogenolysis of C-O bonds. *Chem. Sci.* **10**, 9880–9892 (2019).
41. Li, Y. et al. Mechanistic study of diaryl ether bond cleavage during Palladium-catalyzed lignin hydrogenolysis. *ChemSusChem* doi: 10.1002/cssc.202000753 (2020).
42. Liu, H., Jiang, T., Han, B., Liang, S. & Zhou, Y. Selective phenol hydrogenation to cyclohexanone over a dual supported Pd-Lewis acid catalyst. *Science* **326**, 1250–1252 (2009).
43. Rappoport, Z. The Chemistry of Functional Groups, Wiley-VCH, Weinheim, 2003.
44. Fukuzumi, S. et al. Electron-transfer state of 9-mesityl-10- methylacridinium ion with a much longer lifetime and higher energy than that of the natural photosynthetic reaction center. *J. Am. Chem. Soc.* **126**, 1600–1601 (2004).
45. Kotani, H., Ohkubo, K. & Fukuzumi, S. Photocatalytic oxygenation of anthracenes and olefins with dioxygen via selective radical coupling using 9-mesityl-10-methylacridinium Ion as an effective electron-transfer photocatalyst. *J. Am. Chem. Soc.* **126**, 15999–16006 (2004).
46. Fukuzumi, S., Ohkubo, K. & Suenobu, T. Long-lived charge separation and applications in artificial photosynthesis. *Acc. Chem. Res.* **47**, 1455–1464 (2014).
47. Romero, N. A. & Nicewicz, D. A. Mechanistic insight into the photoredox catalysis of anti-Markovnikov alkene hydrofunctionalization reactions. *J. Am. Chem. Soc.* **136**, 17024–17035 (2014).
48. Romero, N. A., Margrey, K. A., Tay, N. E. & Nicewicz, D. A. Site-selective arene C-H amination via photoredox catalysis. *Science* **349**, 1326–1330 (2015).
49. MacKenzie, I. A. et al. Discovery and characterization of an acridine aadical photoreductant. *Nature* **580**, 76–80 (2020).
50. Fischer, C. & Sparr, C. Configurationally stable atropisomeric acridinium fluorophores. *Synlett* **29**, 2176–2180 (2018).
51. Fischer, C. & Sparr, C. Direct transformation of esters into heterocyclic fluorophores. *Angew. Chem. Int. Ed.* **57**, 2436–2440 (2018).
52. Joshi-Pangu, A. et al. Acridinium-based photocatalysts: a sustainable option in photoredox catalysis. *J. Org. Chem.* **81**, 7244–7249 (2016).
53. Pitzer, L., Sandfort, F., Strieth-Kalthoff, F. & Glorius, F. Carbonyl-olefin cross-metathesis through a visible-light-induced 1,3-diol formation and fragmentation sequence. *Angew. Chem. Int. Ed.* **57**, 16219–16223 (2018).
54. Mandal, S., Chhetri, K., Bhuyan, S. & Roy, B. G. Efficient iron catalyzed ligand-free access to acridines and acridinium ions. *Green Chem.*, **22**, 3178–3185 (2020).
55. Wang, S. F., Cao, X. P. & Li, Y. Efficient aryl migration from an aryl ether to a carboxylic acid group to form an ester by visible-light photoredox catalysis. *Angew. Chem. Int. Ed.* **56**, 13809–13813 (2017).

56. Gonzalez-Gomez, J. C., Ramirez, N. P., Lana-Villarreal, T. & Bonete, P. A photoredox-neutral smiles rearrangement of 2-aryloxybenzoic acids. *Org. Biomol. Chem.* **15**, 9680–9684 (2017).
57. Feng, X., Liao, P., Jiang, J., Shi, J., Ke, Z. & Zhang, J. Perylene diimide based imine cages for inclusion of aromatic guest molecules and visible-light photocatalysis. *ChemPhotoChem* **3**, 1014–1019 (2019).
58. Yang, Q., Jia, Z., Li, L., Zhang, L. & Luo, S. Visible-light promoted arene C–H/C–X lactonization via carboxylic radical aromatic substitution. *Org. Chem. Front.* **5**, 237–241 (2018).
59. Zhang, M., Ruzi, R., Li, N., Xie, J. & Zhu, C. Photoredox and Cobalt co-catalyzed C(sp2)–H functionalization/C–O bond formation for synthesis of lactones under oxidant- and acceptor-free conditions. *Org. Chem. Front.* **5**, 749–752 (2018).
60. Xia, Z. H., Dai, L., Gao, Z. H. & Ye, S. N-heterocyclic carbene/photo-cocatalyzed oxidative smiles rearrangement: Synthesis of aryl salicylates from o-aryl salicylaldehydes. *Chem Commun* **56**, 1525–1528 (2020).
61. Nowada, K., Sakuragi, H., Tokumaru, K. & Yoshida, M. Homolytic aromatic ipso-substitution in aryl ethers by benzoxyl radicals. *Chem. Lett.* 1243–1244 (1976).
62. Adams, G.P., Fine, D.H., Gray, P. & Laye, P.G. Heat of formation of phenyl benzoate and related bond dissociation energies. *J. Chem. Soc. B*, 720–722 (1967).
63. vanScheppingen, W., Dorrestijn, E., Arends, I., Mulder, P. & Korth, H.G. Carbon-oxygen bond strength in diphenyl ether and phenyl vinyl ether: An experimental and computational study. *J. Phys. Chem. A* **101**, 5404–5411 (1997).
64. Ghosh, I., Ghosh, T., Bardagi, J. I. & Konig, B. Reduction of aryl halides by consecutive visible light-induced electron transfer processes. *Science* **346**, 725–728 (2014).
65. Harris, D. C.(ed.) Quantitative Chemical Analysis Ch., W.H. Freeman and Company, New York, 2010, **7**, 142–161.
66. Nicewicz, D., Roth, H. & Romero, N. Experimental and calculated electrochemical potentials of common organic molecules for applications to single-electron redox chemistry. *Synlett* **27**, 714–723 (2015).
67. Cismesia, M. A. & Yoon, T. P. Characterizing chain processes in visible light photoredox catalysis. *Chem. Sci.* **6**, 5426–5434 (2015).

Figures

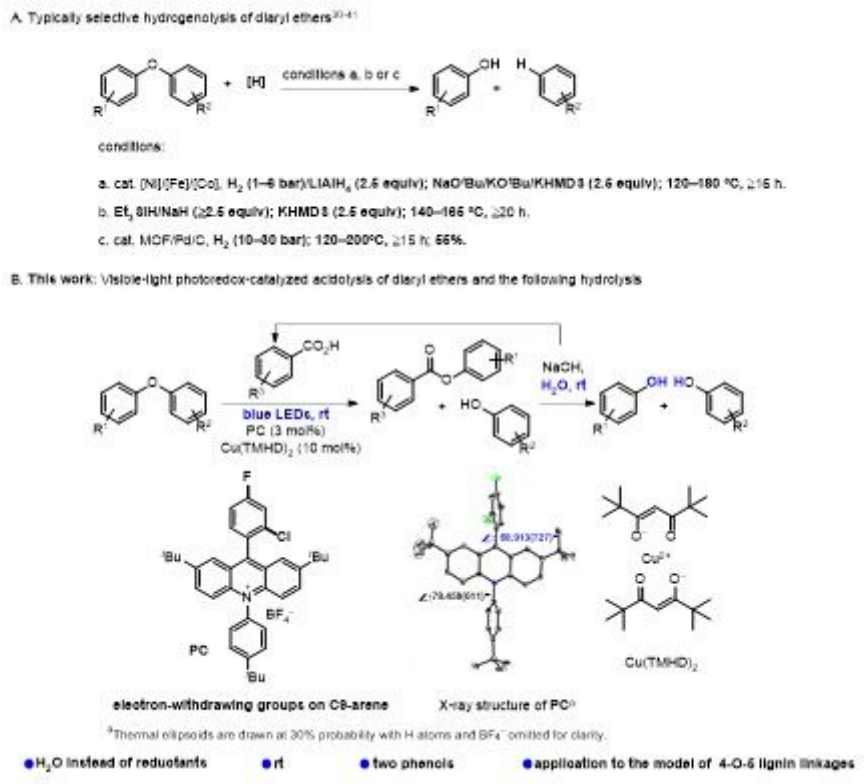

Figure 1

Typically Selective C–O Bond Cleavage of Diaryl Ethers.

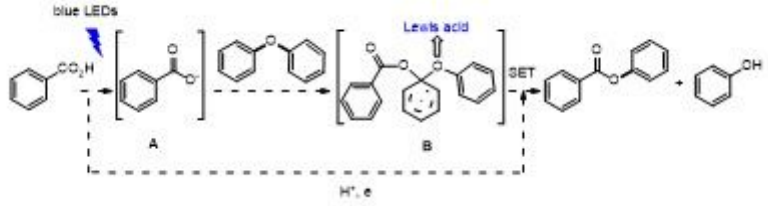

Figure 2

Designed Pathway of Visible-Light Photoredox-Catalyzed Acidolysis of Diaryl Ethers with an aryl carboxylic acid.

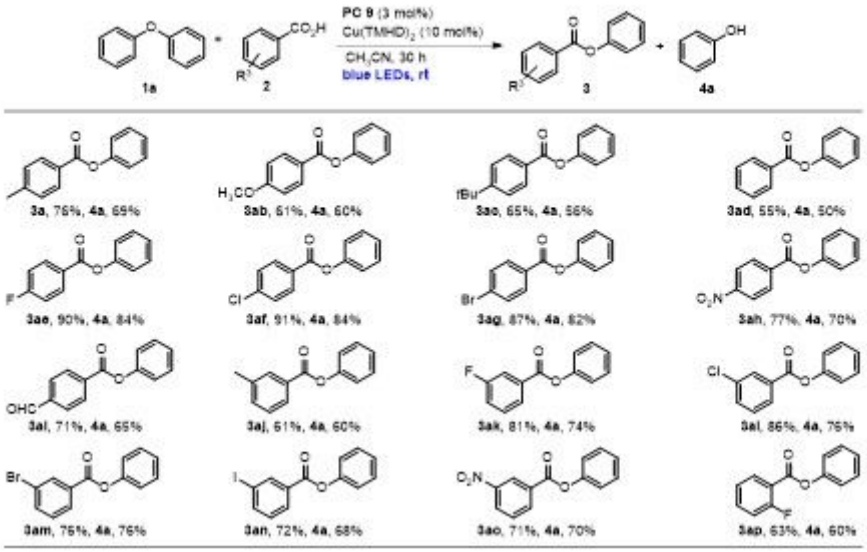

Figure 3

Substrate Scope of Carboxylic Acids. Reaction conditions: 1a (0.50 mmol), 2 (0.60 mmol), PC 9 (3 mol%), Cu(TMHD)2 (10 mol%), CH3CN (5 mL), irradiation with blue LEDs (425-430 nm, 10 W) for 30 h. Isolated yields were reported.

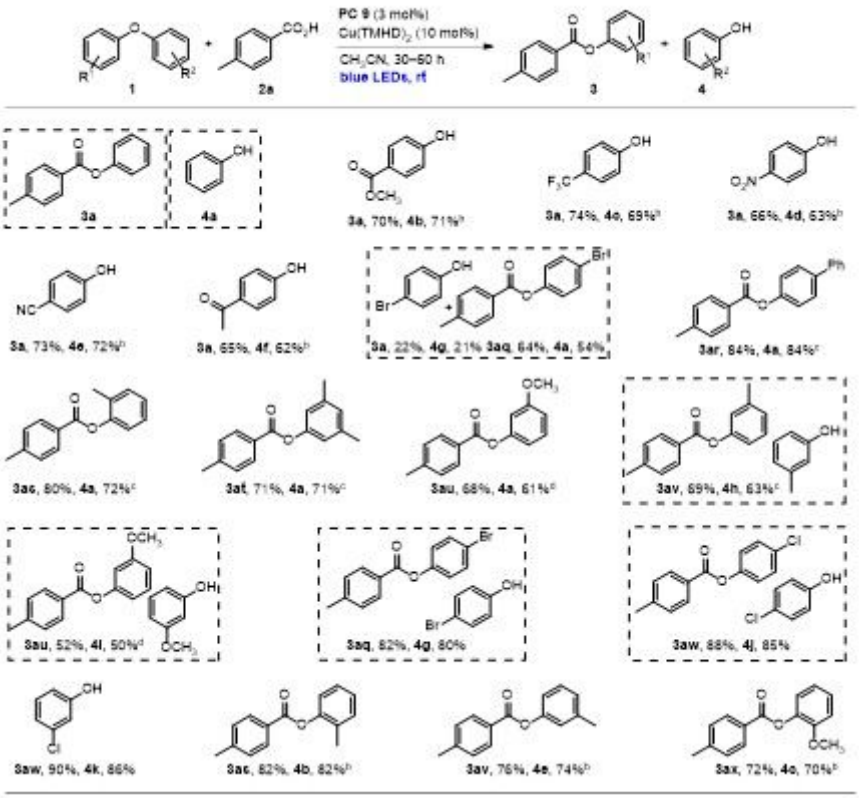

Figure 4

Substrate Scope of Diaryl Ethers. aReaction conditions: 1 (0.5 mmol), 2a (0.6 mmol), PC 9 (3 mol%), Cu(TMHD)2 (10 mol%), CH3CN (5 mL), 30 h. Isolated yields were reported. b60 h. cCH3CN (5 mL) and PhCF3 (2.5 mL), 60 h. d1 (0.2 mmol), 2a (0.24 mmol), PC 9 (3 mol%), Cu(TMHD)2 (10 mol%), CH3CN (2 mL) with PhCF3 (1 mL), stop-flow reactor was used with blue LEDs (420-430 nm, 25 W) irradiation for 60 h.

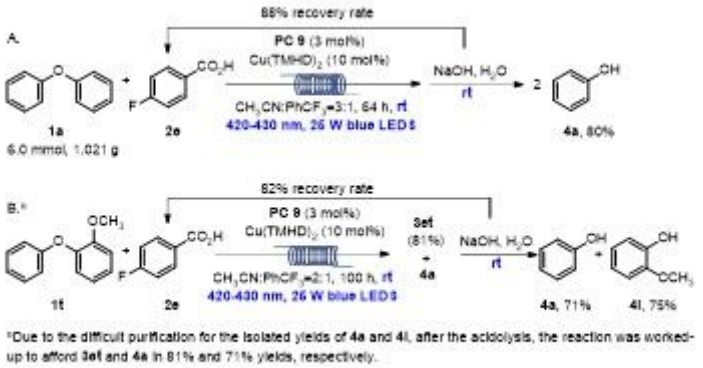

[a]Due to the difficult purification for the isolated yields of 4a and 4l, after the acidolysis, the reaction was worked-up to afford 3el and 4a in 81% and 71% yields, respectively.

Figure 5

Gram-Scale Reaction and Its Application.

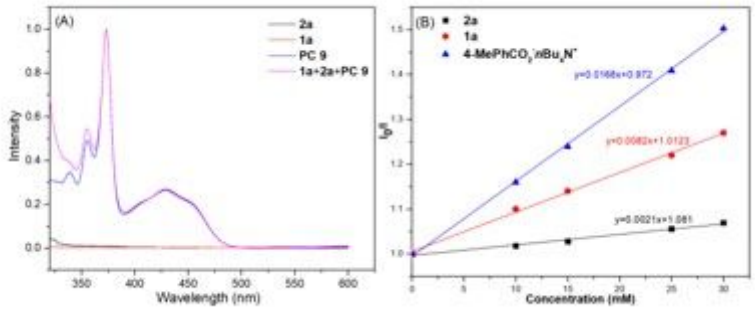

Figure 6

UV-Vis Absorption and Fluorescence Quenching Experiments.

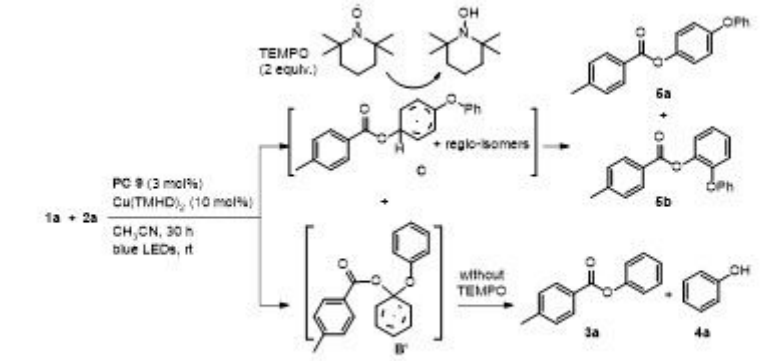

[a]The total isolated yield of 6a and 6b was 37% with the ratio of 5.6:1.0.

Figure 7

Deducing Possible Intermediate B□a.

Figure 8

Proposed Mechanism for the Acidolysis.

Supplementary Files

This is a list of supplementary files associated with this preprint. Click to download.

- SI.pdf